Talanta 175 (2017) 338–346

Contents lists available at ScienceDirect

Talanta

journal homepage: www.elsevier.com/locate/talanta

A novel colorimetric biosensor based on non-aggregated Au@Ag core–shell nanoparticles for methamphetamine and cocaine detection

Kang Mao[a], Zhugen Yang[b], Junrong Li[c], Xiaodong Zhou[c], Xiqing Li[a,*], Jiming Hu[c]

[a] Laboratory for Earth Surface Processes, College of Urban and Environmental Sciences, Peking University, Beijing 100871, China
[b] Division of Biomedical Engineering, School of Engineering, University of Glasgow, Oakfield Road, Glasgow G12 8LT, United Kingdom
[c] Key Laboratory of Analytical Chemistry for Biology and Medicine (Ministry of Education), College of Chemistry and Molecular Sciences, Wuhan University, Wuhan 430072, China

ARTICLE INFO

Keywords:
Au@Ag
Aptamer
Methamphetamine
Colorimetry
Illicit drugs

ABSTRACT

We report a novel colorimetric biosensor based on non-aggregation Au@Ag core-shell nanoparticles to detect methamphetamine and cocaine. The biosensor consisted of a reporter probe (RP) that is a specific single-stranded DNA (ssDNA) sequence coated on Au@Ag nanoparticles, a capture probe (CP) conjugated with magnetic beads, and an illicit drug-binding DNA aptamer (Apt). Au@Ag nanoparticles were synthesized by seed growth and characterized by scanning electron microscope (SEM), high-resolution transmission electron microscopy (HR-TEM), and UV–vis spectra. Methamphetamine (METH) was used as an example to evaluate the feasibility of the biosensor and to optimize the detection conditions. We demonstrated that this sensing platform was able to detect as low as 0.1 nM (14.9 ng L^{-1}) METH with a negligible interference from other common illicit drugs. Various concentrations of METH were spiked into urines, and the biosensor yielded recoveries more than 83.1%. In addition, the biosensor also showed a high sensitivity to detect cocaine. These results demonstrated that our colorimetric sensor holds promise to be implemented as a visual sensing platform to detect multiple illicit drugs in biological samples and environmental matrices.

1. Introduction

Illicit drugs are widely abused and have become an increasing global concern [1–5]. The United Nations Office of Drugs and Crimes has recently reported that illicit drugs had been used by a total of 246 million people, around 5% of the global population aged between 15 and 64 [2]. Among these illicit drugs, cocaine (COC) is the primary drug of concern in Latin America/Caribbean and the second most used illegal substance in both Europe and United States [2,3]. Methamphetamine (METH) is the second most widely abused drug in the world [6]. METH abuse has increased dramatically in the past years particularly in certain regions. For example, crystalline METH seizure has increased from around 7 t in 2010 to 14 t in 2013 in East and Southeast Asia [2]. The abuse of illicit drugs may cause severe societal consequences, such as loss of lives and health of abusers, increased treatment costs, and higher incidence of crimes [1–5].

The commercial analytical techniques include gas chromatography and high performance liquid chromatography-mass spectrometry [4,5]. Although highly sensitive and selective, these techniques usually require expensive instruments and tedious sample pretreatment in laboratory such as solid phase extraction (SPE) or solid phase micro-extraction (SPME). Therefore, there is a great need to develop rapid, inexpensive, and sensitive tools to detect illicit drugs in order to monitor and control illicit drug abuse, preferably on the spot of sample collection.

Compared to conventional methods, biosensors hold promise to overcome the drawbacks of conventional analytical methods. A biosensor is a small device with a biological receptor that generates a signal (electrochemical, optical, nanomechanical, mass sensitive, etc.) in the presence of an analyte. Biosensors have the great potential for rapid and on-site detection of analytes in body fluids and environment samples, due to ease for miniaturization and capability of measuring complex matrices with minimal sample preparation [7–9]. In the past few decades, biosensors have been developed to measure numerous analytes in various matrices, such as heavy metals [10,11], small molecule [12,13], targeted DNA [7], peptides [14], enzyme [15], protein [14,16], antigen [17], biomarkers [7,8] and even bacteria [18,19].

Aptamers have been attracted increasing attentions as a biological receptor for biosensing, which is a sequence of oligonucleotides with high binding affinity and specificity to target utilizing the systematic evolution of ligands by exponential enrichment (SELEX) technology

* Corresponding author.

http://dx.doi.org/10.1016/j.talanta.2017.07.011
Received 26 April 2017; Received in revised form 22 June 2017; Accepted 1 July 2017
Available online 03 July 2017

[20,21]. Recently, efforts have been devoted toward the design of biosensors based on DNA aptamer for the detection of illicit drugs, especially for COC. Most researchers use specific DNA aptamer to bind with COC, which generates a signal (electrochemical [22], colorimetry [23], fluorescence [24], SERS [25], etc.) in the presence of COC due to the conformation changes of DNA aptamers. Mokhtarzadeh et al. [3] reviewed recent advances and applications of COC aptamer-based biosensors and nano-biosensors, which mainly focused on fluorescence, colorimetric and electrochemical techniques for the detection of COC. Besides COC, few other illicit drugs were reported using sensing technology. Mohsen et al. [26,27] firstly developed an electrochemical impedance spectroscopic sensing for methamphetamine using a specific aptamer by SELEX. Shi et al. [6] developed a colorimetric and bare eye determination of urinary methylamphetamine based on aptamers and the salt-induced aggregation of unmodified gold nanoparticles. Yarbakht et al. [28] described the unmodified gold nanoparticles as a colorimetric probe for visual methamphetamine detection.

Nano notable metals, especially gold nanoparticles, have been used increasingly for biosensing application owing to their facile preparation and excellent optical properties [29–31]. These properties are utilized to develop many analytical methods including colorimetry [32,33], light scattering [34,35], scanometry [36,37], surface enhanced Raman scattering [38] and chemiluminescence [39,40]. In particular, colorimetry has particular advantages such as simplicity, low cost, and amenability [32,41]. The nano gold (AuNPs)-based colorimetric biosensor to detect oligonucleotides was first reported by Mirkin's group [29]. In their system, dispersed oligonucleotide-modified AuNPs were assembled into aggregated polymeric networks via hybridization with complementary target sequences. An obvious change in the surface plasmon resonance (SPR) absorption peak between dispersed and aggregated AuNPs was observed, leading to a significant red-to-blue color change which could be easily visualized by naked eyes [29,41]. However, the efficiency of this method to detect lower concentration of targets was limited by the aggregation induced sedimentation [41]. To achieve highly sensitive assay, novel structures of AuNPs have been synthesized [42–44], for example, Au–Ag core–shell plasmonic nanoparticles (PNPs) as molecular probes for the detection of sulfide. This colorimetric assay allows for a linear logarithmic dependence on sulfide concentrations from 50 nM to 100 μM [42]. Yan et al. [43] designed a Au core-Ag shell nanostructures with embedding Cy5-labelled DNA aptamer to target chloramphenicol using surface-enhanced Raman scattering (SERS) for detection. This SERS-based sensor is able to detect as low as 0.19 pg mL^{-1} chloramphenicol. However, Au–Ag core–shell plasmonic nanoparticles (PNPs) have not been used for illicit drug detection.

In this work, we developed a non-aggregated Au@Ag-based colorimetric strategy for illicit drugs detection using a reporter probe, capture probe, and an aptamer. Au@Ag core-shell nanoparticles were synthesized by seeds growth to enhance the SPR signal. The biosensor was optimized by varying the concentrations of magnetic beads and the aptamer, as well as the hybridization reaction time. Selectivity of the sensor was examined using 8 common illicit drugs other than METH. The optimized sensor was used to detect METH in urine specimens of drug addicts to evaluate recovery. This platform was also demonstrated to be capable of detection of other illicit drugs such as cocaine, indicating that it could be used as a generic approach for monitoring of illicit drugs.

2. Materials and methods

2.1. Materials

$HAuCl_4 \cdot 3H_2O$ and $AgNO_3$ were purchased from Shanghai Chemical Reagent Co., Ltd. (Shanghai, China). Carboxyl-coated magnetic beads (1.05 μm Dynabeads™ MyOne™, 10 mg/mL) were purchased from Invitrogen in Norway. Trisodium citrate was obtained from Sigma-Aldrich (USA). Oligonucleotide sequences showed in Table S1 were obtained from Sangon Biotech (Shanghai, China) Co. Ltd. and purified by HPLC. All illicit drugs and metabolites were purchased from Cerilliant (Round Rock, TX, USA). Urines of METH abusers were collected in Guangdong Province with the help of a local rehabilitation center. Urine sample collection and experiments were carried out in accordance with a protocol approved by the ethics committee of Peking University and with informed consent of the addicts. 0.22 μm membrane filters were purchased from ANPEL Laboratory Technologies (Shanghai, China) Inc. Ultra-pure water (18.2 MΩ) from a Millipore filtration system was used in all experiments. Following buffers were used: PB solution (10 mM phosphate sodium buffer solution, pH 7.4), PBS-T buffer (10 mM phosphate sodium buffer solution, pH 7.4, 0.1 M NaCl, 0.05% tween-20), MES buffer (2-[N-morpholino]ethane sulfonic acid, 0.1 M, pH 4.8), and Tris buffer (2-amino-2-hydroxymethyl-1,3-propanediol, 50 mM, pH 7.4).

2.2. Synthesis of Au@Ag core-shell nanoparticles

Gold nanoparticles were prepared by reduction of gold (III) chloride hydrate using trisodium citrate, following the procedure described in a previous publication [45] with minor modifications. Briefly, 50 mL 0.01% (w/w) $HAuCl_4$ was reduced by 750 μL 1% (w/w) trisodium citrate solution at 100 °C under vigorous magnetic stirring for 15–20 min until the solution turned to be light red. The prepared red AuNPs particles were used as seed particles. Then 600 μL of $AgNO_3$ solution (0.5%, w/w) was added to 100 mL boiling gold seed solution. Afterwards, 1 mL sodium citrate solution (1%, w/w) was added dropwise as the reducing agent with stirring. The solution was boiled for 1 h and then cooled down to room temperature. The Au@Ag was characterized by Scanning Electron Microscope (SEM) (SIGMA, Germany), Transmissions Electron Microscope (TEM) (JEM-2100) and UV–vis spectrometer (Perk Elmer, USA), which confirms the successful synthesis of Au@Ag core-shell nanoparticles with a mean diameter of 40 nm.

2.3. Preparation of reporter and capture probe

The reporter probe was derived by modifying the synthesized Au@Ag core-shell nanoparticles with a RP DNA sequence that was partially complementary to the aptamer. The Au@Ag core-shell nanoparticles suspended in 5 mL PB buffer (pH 7.4, 10 mM phosphate) were loaded with 15 nmol thiol-functionalized reporter probes [46]. After 24 h, 2 M NaCl was added to the solution to generate an overall NaCl concentration at 0.05 M, and then increased to 0.1 M after standing for 8 h. Upon aging in 0.1 M salt for additional 40 h, the nanoparticles were isolated by centrifugation at 6500 rpm for 15 min and washed three times with PBS-T (pH 7.4, 10 mM phosphate, 0.05% Tween-20).

The capture reporter was super paramagnetic magnetic beads (MBs) with a carboxyl-modified coating, which were conjugated with the capture probe DNA using the protocol suggested by the manufacturer. Before immobilization, 2.5 mL of carboxylated magnetic beads were washed twice with 2.5 mL of MES buffer (100 mM, pH 4.8) and then resuspended in 250 μL MES buffer (100 mM, pH 4.8). Next, a mixture of 36.2 nmol NH_2-modified capture DNA and 36.2 μmol EDC•HCl in 100 μL MES buffer was added to the washed magnetic beads and incubated overnight with gently shaking at room temperature. Finally, the coated MBs were incubated with 50 mM Tris buffer (pH 7.4) for 15 min at room temperature with gentle shaking to quench the remaining activated carboxylic acid groups. The coated magnetic beads were washed for three times with 2.5 mL Tris buffer and then resuspended in hybridization buffer (PBS-T) and stored at 4 °C for use.

2.4. Elaboration of biosensors

In this study, we try to develop a strategy for illicit drugs detection

based on the non-aggregated Au@Ag. To explore the effectiveness of the strategy, a non-aggregated Au@Ag nanoprobes-based on METH was employed as a case study. METH (1 μM, 10 μL) was mixed with 10 μL METH aptamer (200 nM) solutions, followed by introducing 20 μL PBS-T buffer. After incubation for half an hour, 5 μL CP (PBS-T buffer) and 50 μL RP (PBS-T buffer) were then added to the solution and allowed to hybridize under gently vortexing for 90 min. The total volume was increased to 100 μL in PBS-T buffer. After hybridization, the MBs with target-linked Au@Ag core-shell nanoparticles together with unreacted MBs were easily attracted to the bottom of the tube by applying a round magnet (diameter: 3 cm, thickness: 3 mm). After the separation, the SPR of the supernatant was measured by a Shimadzu UV-2550 with 80 μL quartz micro-cuvette.

Control experiments were performed with following combinations: MBs + Au@Ag; MBs + Au@Ag + METH; MBs + Au@Ag + aptamer. In these experiments, each component was added at the same volumes and concentrations as in the presence of METH. The missing components were replaced by the PBS-T buffer to maintain a constant total volume (100 μL).

2.5. Optimization of biosensors

The concentration of magnetic beads causes the change of the ratio between the capture probes and reporter probe, which has significant impacts on the sensitivity of the assay. In order to get the optimal concentration of magnetic beads, a series of MBs concentrations were tested in this experiment. The experimental process was the same as the control experimental procedure (MBs + Au@Ag + aptamer) mentioned above. The volume of MBs (10 mg/mL) was 0, 0.1 μL, 0.5 μL, 1, and 5 μL.

The hybridization reaction time is an important parameter for colorimetric biosensor. We examined the reaction time of the hybridization by recording the peak intensities of SPR signal. The experimental process was also the same as the control experimental procedure described above. SPR signals were recorded every 15 min from 0 to 105 min.

The optimal concentration of METH aptamer was determined by measuring absorbance intensities at 400 nm. The biosensor was optimized using different concentrations of aptamer (0, 10 nM, 20 nM, 30 nM, 40 nM, 50 nM, and 60 nM), following the procedure for control experiments mentioned above.

2.6. Evaluation of the analytical performance

Under the optimized conditions, the sensitivity and linearity of the biosensor for METH were evaluated from 0.50nM to 200 nM.

The **s**electivity of the biosensor was evaluated by other 8 common illicit drugsand metabolites, namely ketamine (KET), norketamine (NK), morphine (MOR), cocaine (COC), cathinone (CAT), methcathinone (MCAT), 3-trifluoromethyphenylpiperazine (BZP), and 4,4′- two amino two phenyl methane (MDA). The experiment procedure was same as above, except that METH was replaced by other illicit drugs or metabolites. A much higher concentration (1 μM) was used for other drugs and metabolites, whereas a METH concentration of 50 nM was used as control.

2.7. Analysis of urine samples with biosensors

To test the feasibility of detecting METH in biological samples, METH concentrations in urines were determined using the biosensor. An aliquot of 20 μL of each urine samples were measured using our sensors after filtered with 0.22 μm membrane filters. The measured concentrations were compared with those determined from high performance liquid chromatography-tandem mass spectrometer (HPLC-MS/MS) used a UFLCXR-LC system (Shimadzu, Japan) with a Phenomenex Gemini C18 column (100 mm 2 mm, 3 μm) and an ABI 4000 triple quadrupole mass spectrometer (AB SCIEX, USA). For HPLC-MS/MS analysis, the urine samples were first diluted by MeOH by a factor of 6, vortexed for 20 s, and centrifuged for 1 min at 13,000 rpm. Aliquots of supernatants, added with deuterated internal standards analyzed following conditions described elsewhere [4,5]. To examine the recovery of METH, one of the urine samples was spiked with three concentrations (10, 50, and 100 nM). The METH concentrations in spiked samples were then determined using the biosensor.

2.8. Cocaine detection with biosensors

In order to explore the universal applicability of our proposed strategy, another widely-used illicit drug, cocaine, was detected with the same approach. The detection followed the conditions for METH except with minor changes as follows: 1) the concentration of cocaine (COC) in the initial detection experiment and control experiment was 150 nM; 2) COC aptamer concentrations of 0, 5, 10,15, 20, 30, 40, and 50 nM were tested to find the optimal concentration; 3) COC concentrations 0, 0.5, 1.0, 5.0, 10.0, 20.0, 40.0, 60.0, 80.0, 100.0, and 150.0 nM were tested to examine the sensitivity and linearity of the biosensor.

3. Results and discussion

3.1. Characteristics of Au@Ag

According to experimental results, a significant red-to-yellow color change between AuNPs and Au@Ag can be easily visualized by the naked eye. Fig. 1A showed that the average diameter of Au@Ag core-shell nanoparticle was approximately 40 nm. Furthermore, the contrast of the shell-silver nano particles is different from that of the core-AuNP in HR-TEM image (Fig. 1B). The analysis of the UV–vis spectra (Fig. 1 C) from AuNPs and Au@Ag core-shell nanoparticles show that the absorption peak (λ_{max}) shifted from 520 nm to 400 nm, indicating a blue shift. This is because AuNPs and Au@Ag have different frequencies of surface plasmon resonance (SPR) in spite of the same particle size. The shift in the SPR absorption peak between AuNPs and Au@Ag led to the significant red-to-yellow color change. The intensity of SPR signal from Au@Ag was much stronger than that from AuNPs even though at the same concentrations. Thus, Au@Ag is a better signal transducer compared to AuNPs.

3.2. Feasibility of biosensor

The designed mechanism of the new colorimetric sensor is illustrated in Scheme 1. The biosensor consisted of a reporter probe (RP) (Scheme 1A), a capture probe (CP) (Scheme 1B) and an aptamer (Apt). The reporter probe was derived by modifying the synthesized Au@Ag core-shell nanoparticles with a RP DNA sequence that was partially complementary to the aptamer (Scheme 1A). The capture reporter was super paramagnetic magnetic beads (MBs) with a carboxyl-modified coating, which can be functionalized with amine-modified oligonucleotides with 1-ethyl-3-(3-dimethylaminopropyl) carbodiaimide hydrochloride (EDC•HCl) as the linker (Scheme 1B). The amine-modified oligonucleotides are able to fully match one portion of a target sequence but are different from the fragment complementary with RP DNA. And these MBs were attracted by an external magnetic field and facilitate the sample separation activated by an external magnetic field. As is shown in Scheme 1C, the aptamer could bind to reporter probe and capture probe to form Au@Ag-DNA-MBs sandwich structure through hybridization. The double-stranded DNA (dsDNA) was composed of both RP DNA and CP DNA complementary to the different DNA aptamer fragment. When an external magnetic field is applied, the sandwich structure complex is removed from the suspension, which reduces the intensity of SPR signal from Au@Ag core-shell nanoparticles [47,48]. In contrast, in the presence of the target drugs,

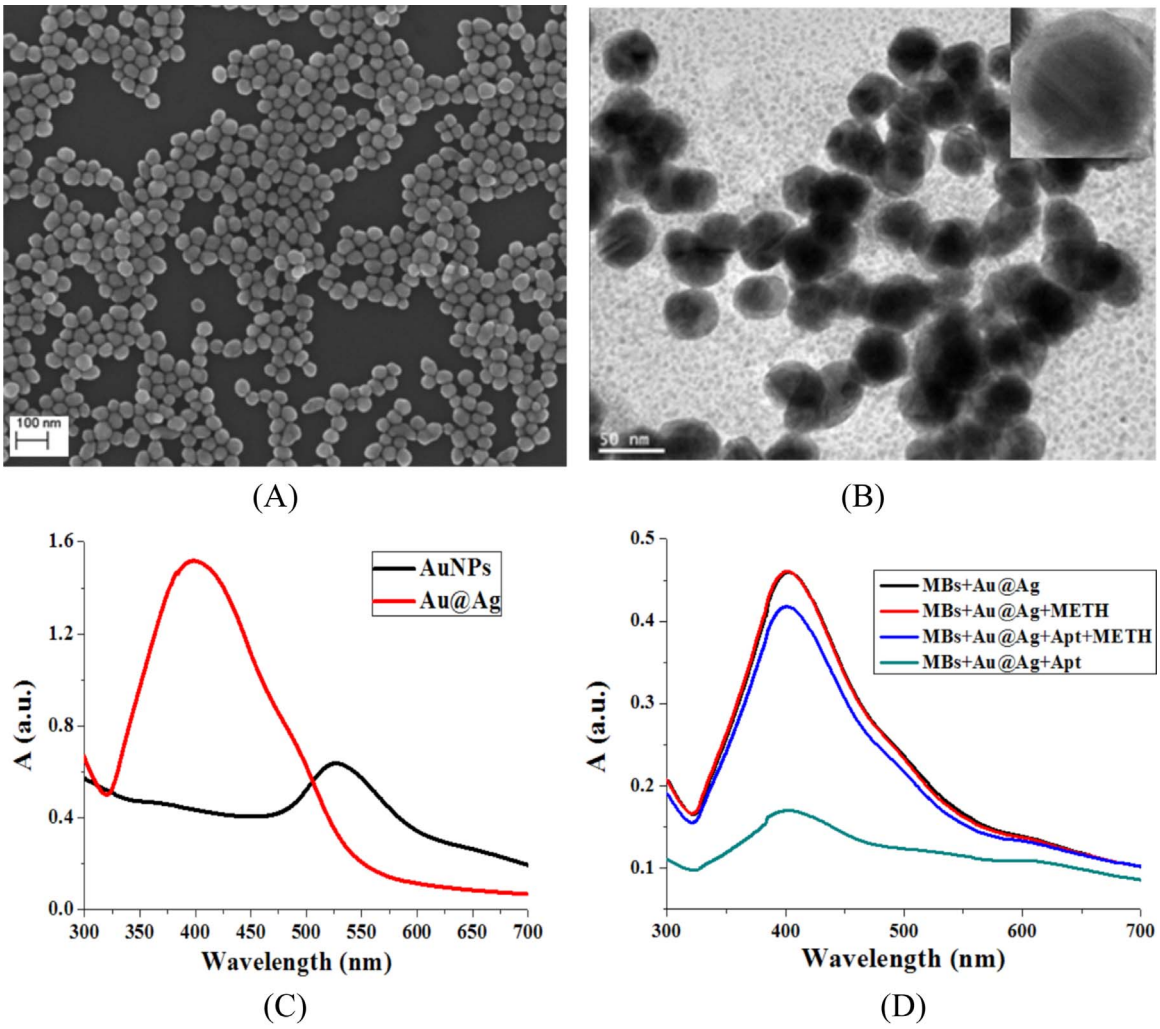

Fig. 1. (A) Scanning electron microscope (SEM) image and (B) high resolution transmission emission microscope (HR-TEM) image of prepared Au@Ag core–shell nanoparticles. (C) SPR signal of Au@Ag and AuNPs. (D) UV–vis spectra of Au@Ag in the presence or absence of METH. The signal (A) is the absorbance of Au@Ag core-shell nanoparticles and error bars represent triplicate measurements (same for below).

aptamer binding to the two probes is prevented and Au@Ag-DNA-MBs complex cannot be formed the aptamer which binds preferably with the target drug molecules due to higher affinity [26,27]. Thus, the concentration of Au@Ag remaining in the supernatant is proportional to the concentrations of target drugs. As the amount of the target drug increased, the color of the supernatant changed from light yellow to deep yellow, which could be measured with UV–vis spectrometer and even be visualized by naked eye.

To test the feasibility of this strategy, effects of this analytical method with or without illicit drugs (e.g. METH) on the SPR signal of Au@Ag core-shell nanoparticles were determined. In the control experiment, an absolute absorbance intensity of 0.46 was observed (Fig. 1D, MBs+Au@Ag). When METH was added to the system, the absorbance intensity has no significant change (Fig. 1D, MBs+Au@Ag +METH), indicating that METH alone had no interference to this analytical system. When METH aptamer was added to the system, the absorbance intensity decreased dramatically (Fig. 1D, MBs+Au@Ag +Apt), due to the formation of the Au@Ag-dsDNA-MBs complex following the base pair matching principle to form dsDNA. The Au@Ag-dsDNA-MBs sandwiches could be removed by external magnetic field. The removal of Au@Ag core-shell nanoparticles leaded to a decrease in absorbance signal at 400 nm. When both METH and METH aptamer existed in this system, the absorbance was basically recovered (Fig. 1D, MBs+Au@Ag+Apt+METH). The signal was only slightly lower than the value of absolute absorbance intensity of Au@Ag core-shell nanoparticles. The increase in absorbance in the presence of both METH aptamer and METH was due to formation of METH-aptamer complex. The complex blocked formation of the Au@Ag-DNA-MBs complex, which prevented removal of the Au@Ag core-shell nanoparticles by the external magnetic field.

According to our experimental results, (1) The color of the solution is always yellow and can only be reduced in magnitude in the presence of different concentration of METH (Fig. 3C); (2) There is no complex spectrum in the presence of different concentration of METH (Fig. 3A); (3) The peak of SPR signal is always at 400 nm, thus, there is no red shift or blue shift (Fig. 3A). Thus, on this sensing platform, Au@Ag core-shell nanoparticles would bind specifically with magnetic particles without the formation of the Au@Ag aggregates. This simple design avoids the complex spectrum of the classical colorimetric biosensor based on nanoparticles aggregation [6]. The color of the solution is always yellow and can only be reduced in magnitude. Due to the stability of dispersed Au@Ag core-shell nanoparticles, one only needs to examine the change in intensity of their specific absorption peak rather than the complex spectra of aggregates. These results indicate that designed mechanism is effective to detect METH.

3.3. Optimization of sensing conditions

The concentration of magnetic beads has a significant effect on experimental result. Excessive magnetic beads would cause waste,

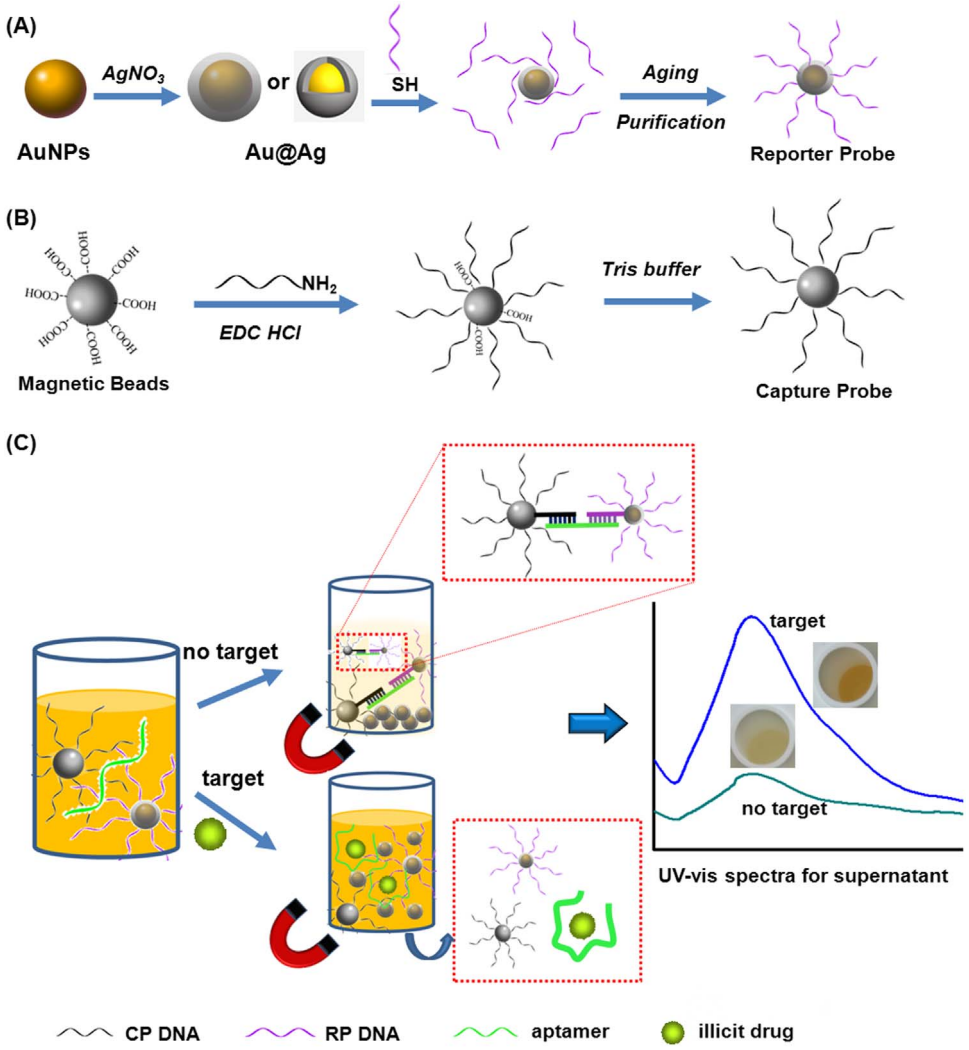

Scheme 1. The schematic representations of preparation of reporter probe (A) and capture probe (B) and colorimetric detection of illicit drug based on non-aggravation Au@Ag core-shell nanoparticles (C).

whereas insufficient magnetic beads would have a significant impact on the sensitivity of biosensors. In order to get the optimal concentration of magnetic beads, sensitivity of colorimetric approach in the presence of various MBs was also monitored, and the minimum SPR signal was optimized as the experimental condition. The optimized concentration of the MBs was determined with unchanged concentration of reporter probes and METH aptamer. As shown in Fig. 2A, optimized MBs volume to achieve the highest sensitivity was around 1 μL.

The hybridization time to form Au@Ag-dsDNA-MBs is an important parameter for the evaluation of colorimetric approach. Aptamers were added at the time point of 0 s, and spectra changes were observed. After addition of the METH aptamer, the SPR peak signals of Au@Ag core-shell nanoparticles were recorded for 110 min Fig. 2B shows that the intensity of SPR signal at 400 nm gradually decreased, and reached the minimum value in about 60 min. So the optimal reaction time is 60 min.

SPR signal of Au@Ag nanoparticles decreased with increasing concentrations of METH aptamer (Fig. 2C). Near completely quenching occurred at a concentration of 60 nM. It should be noted that the excessive usage of METH aptamer could result in non-specific (i.e., no SPR enhancement) binding to the METH. As shown in Fig. 2C, at an aptamer concentration of 40 nM, METH prevented the quenching of the Au@Ag and SPR intensity of Au@Ag was almost fully recovered (up to 89.1%) to its initial value. Thus, 40 nM METH aptamer was optimised for our biosensor.

3.4. Evaluation of sensing performance

To determine the limit of detection (LOD) of our biosensors, different concentrations of METH from 0 to 200 nM were measured. Fig. 3A shows the dose response of METH concentration with the colorimetric signal. As the METH concentrations increasing, the color of the supernatant solution turned from light yellow and to deep yellow (Fig. 3C). The peak intensity of SPR signal is proportional to METH concentration, and the increasing METH concentration therefore leads to the deformation of Au@Ag-DNA-MBs sandwich structure. As is shown in Fig. 3B, the intensity of SPR signal (λ_{max} = 400 nm) increased with the increasing METH concentrations, and the linear range was determined from 0.5 to 200 nM (R^2 = 0.994). The LOD of the biosensor was determined to be 0.1 nM (3σ), which is much lower than 1000 ng mL^{-1} (6.7 μM), the threshold of positive METH detection in urine samples recommended by the National Institute on Drug Abuse of United States [49]. Shi et al. developed a aptamer biosensor for the detection of METH based on gold nanoparticles with a LOD at 0.82 μM [6]. Oghli et al. is able to electrochemically detect METH as low as 50 nM [50]. Compared to those sensors, our sensitivity is much improved and holds a great potential for routine screening of METH in urine samples

To examine the selectivity of our biosensor, other 8 illicit drugs and/or metabolites (KET, NK, MOR, COC, CAT, MCAT, BZP, and MDA) were tested. Fig. 4A showed the responses of the colorimetric

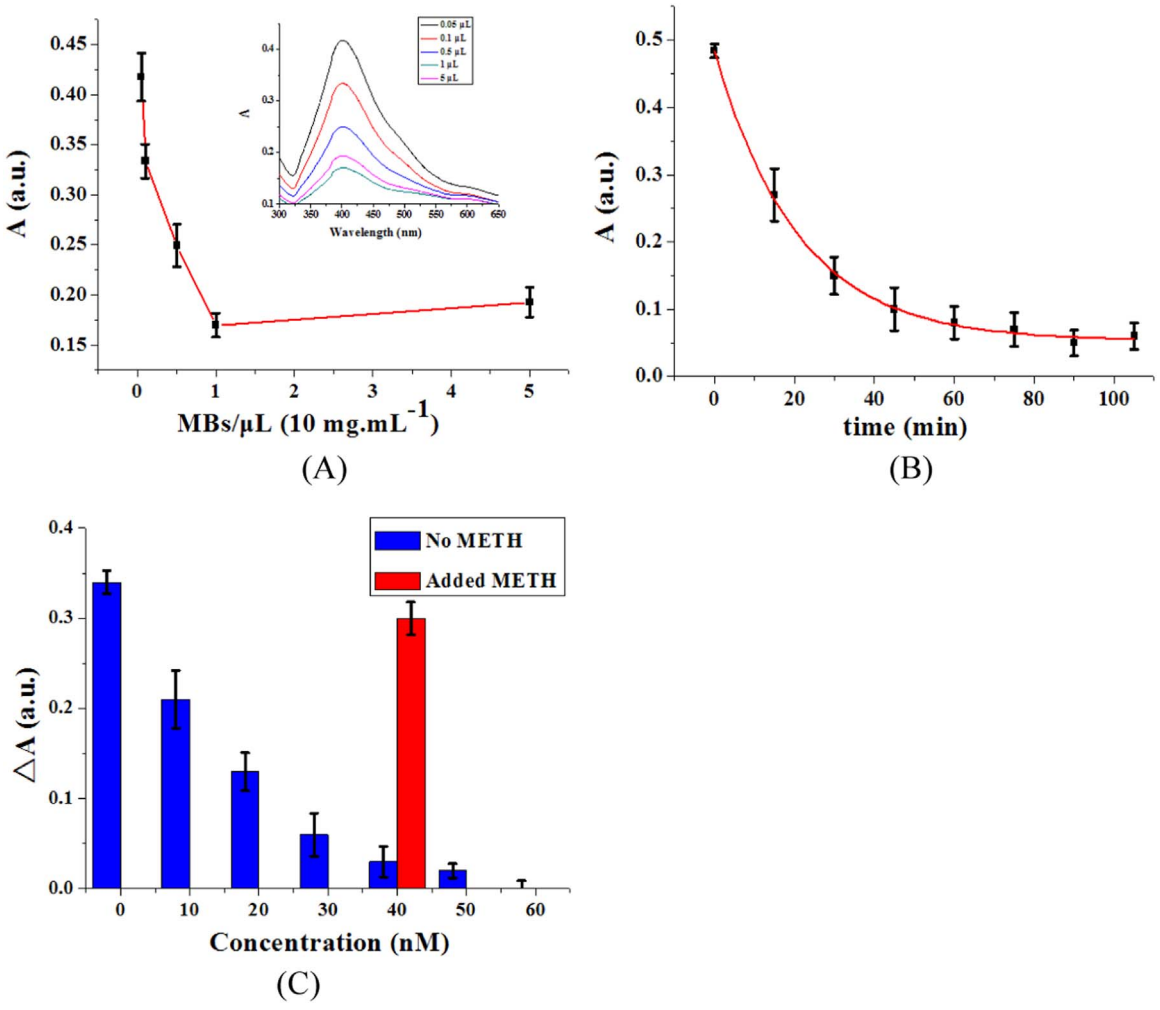

Fig. 2. (A) SPR signal intensities at different MBs concenctrations. The curve and UV–vis spectra (insert) of the supernatant at different concentrations of MBs. Under the same concentration of METH aptamer (40 nM), the sensitivity of assay positively correlated with variation of SPR peak intensity. (B) Hybridization reaction time of SPR signal intensity change at 400 nm with METH aptamer concentration of 40 nM. (C) SPR signal intensities of the Au@Ag (λ_{max} = 400 nm) in the presence of different concentrations of METH aptamer (Blue). Red bar is SPR signal intensity of the Au@Ag in the presence of METH (100 nM). The signal (ΔA) is expressed as the relative absorbance with respect to the blank and error bars represent three replicate measurements (same for below).

assay of METH (50 nM) and other drugs or metabolites (1 μM) under the optimized condition. METH led to an evident increase in the 400 nm value of the assay. In contrast, the absorbance signals associated with others compounds stayed at the same level as the blank. These signals were much lower than that in the presence of METH, despite the fact that METH concentration (50 nM) was much lower than other illicit drugs and/or metabolites. Furthermore, the enhancement in absorbance signals (relative to the blank) was not statistically significant among other drugs, These results demonstrate that binding affinity of METH to METH-aptamer were much stronger than that to all other illicit drugs, rendering the biosensor with high specificity toward METH.

In order to further investigate the potential application of the proposed sensor, the assay was employed to detect METH in urine samples. The average recovery of METH in spiked urine sampled ranged from 83.1% and 90.5% (Table 1). The METH concentrations measured using HPLC-MS/MS (Fig. 4B, black bar) ranged from 19.2 to 131.8 nM. METH concentrations (Fig. 4B, red bar) analyzed using our biosensor fell within the same range, but were slightly lower than the HPLC-MS/MS-derived concentrations, probably due to matrix effect [4,51–53]. The variation of the measured value from our sensors and HPLC-MS/MS are less than 8.7%, indicating that our sensors have a clear potential for the detection of METH in real biological samples.

3.5. Detection of cocaine with biosensors

The sensing platform was also used to detect cocaine to explore the feasibility of this strategy as a generic platform. The probe sequences (Table. S1) are composed of an aptamer for COC and two probes that are complementary to the cocaine aptamer in different regions. As expected, in the absence of COC, the SPR signal of the supernatant was much lower than absolute SPR signal of Au@Ag; however, in the presence of COC, the strong SPR signal nearly equal to the absolute SPR signal of Au@Ag was observed (Fig. S2). Optimal concentration of COC aptamer was found to be 30 nM, which is less than that of METH aptamer (Fig. S3). Furthermore, a log-linear relationship (R^2 = 0.987) between COC concentration and absorbance signal intensity was also observed in a COC concentration range from 1.0nM to 150 nM. The LOD was 0.5 nM (Fig. S4), lower than previously reported value [23]. The promising results clearly demonstrate the versatility of the non-aggregation Au@Ag colorimetric strategy for illicit drug detection.

4. Conclusion

A novel, cost-effective and label-free biosensor based on the non-aggregation Au@Ag was constructed for illicit drugs detection. The biosensor consisted of a reporter probe that is a specific single-stranded DNA sequences coated with Au@Ag, a capture probe conjugated with

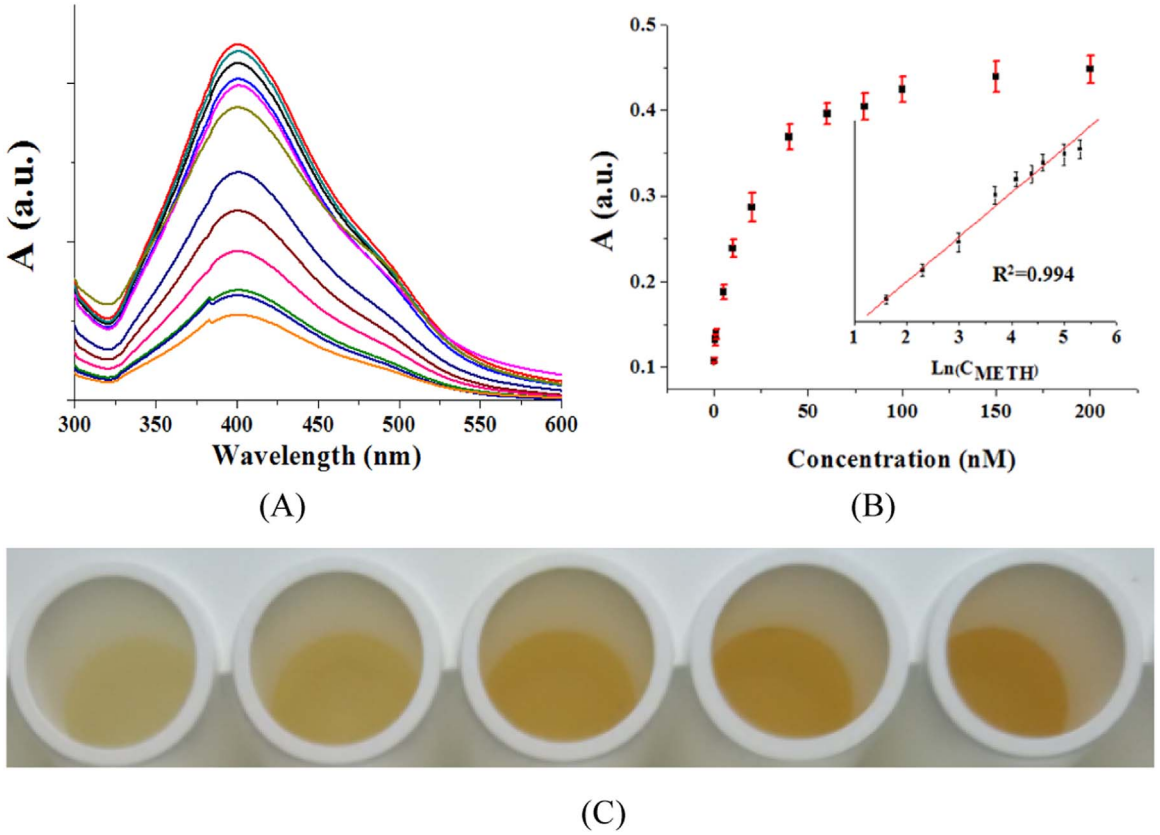

Fig. 3. (A) UV–vis spectra of Au@Ag in the presence of different concentrations of METH (from bottom to up: 0, 0.5, 1, 5, 10, 20, 40, 60, 80, 100, 150, 200 nM). (B) SPR signal intensity (λ_{max} = 400 nm) at various METH concentrations (The inset shows the logarithm linear range concentration (0.5–200.0 nM). (C) Color change of the non-aggravation Au@Ag in the presence of METH. The METH concentrations in tubes from left to right were: 0, 5, 10, 50, and 100 nM.

superparamagnetic magnetic beads, and an illicit drug-binding DNA aptamer. The DNA aptamer could hybridize with both RP and CP, generating Au@Ag-DNA magnetic beads (MBs) sandwich structure. When an external magnetic field is applied, Au@Ag-DNA-MB is removed from the solution, leading to decreased SPR intensity. In the presence of the illicit drugs, Au@Ag-DNA-MB sandwich structure cannot be formed due to higher affinity of the aptamer to illicit drug than that to complementary ssDNA. The SPR intensity is correlated with the concentrations of target illicit drugs and used to quantify the target drugs. We demonstrated the novel sensing platform for the detection of illicit drugs such as METH and COC.

The optimized biosensor is able to detect as low as 0.1 nM METH with a linear range of from 0.5nM to 200 nM, and other non-specific illicit drugs show a negligible interference. Recoveries of METH in the spiked urine samples were evaluated to be more than 83.1%. We also use HPLC-MS/MS to analyze urine samples for the validation, and the results are in agreement. Furthermore, the developed sensing platform was used for the detection of cocaine with the cocaine-binding aptamer, which shows a promising result and the universality of our biosensors. In summary, we have demonstrated a generic biosensor based on non-aggregation Au@Ag core-shell structure for the sensitive detection of METH and COC, and it also has a potential for monitoring a wide

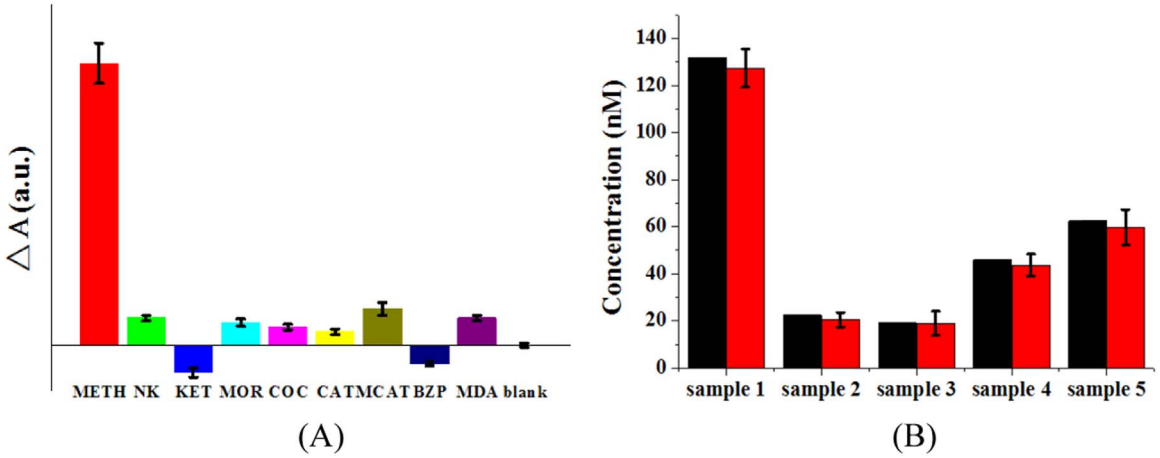

Fig. 4. (A) Selectivity of the non-aggravation Au@Ag core-shell nanoparticles for METH detection. The METH concentration was 50 nM, while the concentration of other illicit drugs was 1 μM. From left to right: METH, KET, NK, MOR, COC, CAT, MCAT, BZP, MDA, and blank; (B) METH concentrations in human urine samples measured by the biosensor and (red) and by HPLC-MS/MS (black). (For interpretation of the references to color in this figure legend, the reader is referred to the web version of this article.)

Table 1
Recovery of METH in urines at three spiked METH concentration (10.0, 50.0 and 100.0 nM), respectively.

Spiked concentration (nM)	The measured concentration of METH (nM)				Rate of standard recovery (%)			
	1	2	3	Average	1	2	3	Average
0	19.23	18.74	18.85	18.94	–	–	–	–
10	27.35	27.75	26.64	27.25	81.2	90.1	77.9	83.1
50	64.30	59.30	65.80	63.13	90.1	81.1	93.9	88.4
100	113.40	109.50	105.30	109.40	94.2	90.8	86.5	90.5

spectrum of targets including illicit drugs by replacing respective DNA aptamer.

Acknowledgments

We gratefully acknowledge the support from the National Natural Science Foundation of China (NSFC) (Nos. 41371442 and 41401566).

Appendix A. Supplementary material

Supplementary data associated with this article can be found in the online version at doi:10.1016/j.talanta.2017.07.011.

References

[1] S. Galanie, K. Thodey, I.J. Trenchard, I.M. Filsinger, C.D. Smolke, Complete biosynthesis of opioids in yeast, Science 349 (6252) (2015) 1095–1100.
[2] United Nations Office of Drugs and Crime, World Drug Report 2015, 2015.
[3] A. Mokhtarzadeh, J.E.N. Dolatabadi, K. Abnous, M.D.L. Guardia, M. Ramezani, Nanomaterial-based cocaine aptasensors, Biosens. Bioelectron. 68 (68) (2015) 95–106.
[4] P. Du, K. Li, J. Li, Z. Xu, X. Fu, J. Yang, H. Zhang, X. Li, Methamphetamine and ketamine use in major Chinese cities, a nationwide reconnaissance through sewage-based epidemiology, Water Res. 84 (2015) 76–84.
[5] B. Subedi, K. Kannan, Mass loading and removal of select illicit drugs in two wastewater treatment plants in New York State and estimation of illicit drug usage in communities through wastewater analysis, Environ. Sci. Technol. 48 (12) (2014) 6661–6670.
[6] Q. Shi, Y. Shi, Y. Pan, Z. Yue, H. Zhang, C. Yi, Colorimetric and bare eye determination of urinary methylamphetamine based on the use of aptamers and the salt-induced aggregation of unmodified gold nanoparticles, Microchim. Acta 182 (3–4) (2015) 505–511.
[7] Z. Yang, M.A. D'Auriac, S. Goggins, B. Kasprzyk-Hordern, K.V. Thomas, C.G. Frost, P. Estrela, A novel DNA biosensor using a Ferrocenyl Intercalator applied to the potential detection of human population biomarkers in wastewater, Environ. Sci. Technol. 49 (9) (2015).
[8] R.D.L. Rica, M.M. Stevens, Plasmonic ELISA for the ultrasensitive detection of disease biomarkers with the naked eye, Nat. Nanotechnol. 7 (12) (2012) 821–824.
[9] Z. Yang, B. Kasprzyk-Hordern, C.G. Frost, P. Estrela, K.V. Thomas, Community sewage sensors for monitoring public health, Environ. Sci. Technol. 49 (10) (2015) 5845–5846.
[10] K. Mao, Z. Wu, Y. Chen, X. Zhou, A. Shen, J. Hu, A novel biosensor based on single-layer MoS2 nanosheets for detection of Ag+, Talanta 132 (2015) 658–663.
[11] F.W. †, R.O. †, I. Willner, Detection of metal ions (Cu 2+, Hg 2+) and cocaine by using ligation DNAzyme machinery, Chem. Eur. J. 18 (50) (2012) 16030–16036.
[12] Q. Li, Y.D. Wang, G.L. Shen, H. Tang, R.Q. Yu, J.H. Jiang, Split aptamer mediated endonuclease amplification for small-molecule detection, Chem. Commun. 51 (20) (2015) 4196–4199.
[13] M.A.D. Neves, C. Blaszykowski, S. Bokhari, M. Thompson, Ultra-high frequency piezoelectric aptasensor for the label-free detection of cocaine, Biosens. Bioelectron. 72 (2015) 383–392.
[14] A.B. Iliuk, L. Hu, W.A. Tao, A. Chem, Aptamer in bioanalytical applications, Anal. Chem. 83 (12) (2011) 4440–4452.
[15] Z. Wu, Y. Liu, X. Zhou, A. Shen, J. Hu, A "turn-off" SERS-based detection platform for ultrasensitive detection of thrombin based on enzymatic assays, Biosens. Bioelectron. 44 (2013) 10–15.
[16] J. Das, K.B. Cederquist, A.A. Zaragoza, P.E. Lee, E.H. Sargent, S.O. Kelley, An ultrasensitive universal detector based on neutralizer displacement, Nat. Chem. 4 (8) (2012) 642–648.
[17] M.A. Najeeb, Z. Ahmad, R.A. Shakoor, A.M.A. Mohamed, R. Kahraman, A novel classification of prostate specific antigen (PSA) biosensors based on transducing elements, Talanta 168 (2017) 52–61.
[18] K. Saha, S.S. Agasti, C. Kim, X. Li, V.M. Rotello, Gold nanoparticles in chemical and biological sensing, Chem. Rev. 112 (5) (2012) 2739–2779.
[19] P.D. Howes, R. Chandrawati, M.M. Stevens, Colloidal nanoparticles as advanced biological sensors, Science 346 (6205) (2014).
[20] S.M. Shamah, J.M. Healy, S.T. Cload, Complex target SELEX, Acc. Chem. Res. 41 (1) (2008) 130–138.
[21] N. Duan, W. Gong, S. Wu, Z. Wang, Selection and Application of ssDNA Aptamers against Clenbuterol Hydrochloride Based on ssDNA Library Immobilized SELEX, J. Agr. Food Chem. 65 (8) (2017) 1771–1777.
[22] Z. Yang, E. Castrignanò, P. Estrela, C.G. Frost, B. Kasprzyk-Hordern, Community sewage sensors towards evaluation of drug use trends: detection of cocaine in wastewater with DNA-directed immobilization aptamer sensors, Sci. Rep. 6 (2016).
[23] M.N.S, D.W. Landry, Aptamer-based colorimetric probe for cocaine, J. Am. Chem. Soc. 124 (33) (2002) 9678–9679.
[24] M.N. Stojanovic, P.D.P, D.W. Landry, Aptamer-based folding fluorescent sensor for cocaine, J. Am. Chem. Soc. 123 (21) (2001) 4928–4931.
[25] M. Oroval, M. Coronado-Puchau, J. Langer, M.N. Sanz-Ortiz, Á. Ribes, E. Aznar, C. Coll, M.D. Marcos, F. Sancenón, L.M. Liz-Marzán, Surface enhanced Raman scattering and gated materials for sensing applications: the ultrasensitive detection of mycoplasma and cocaine, Chem. Eur. J. (2016).
[26] M. Ebrahimi, M. Johariahar, H. Hamzeiy, J. Barar, O. Mashinchian, Y. Omidi, Electrochemical impedance spectroscopic sensing of methamphetamine by a specific aptamer, Bioimpacts Bi 2 (2) (2012) 91–95.
[27] M. Ebrahimi, H. Hamzeiy, J. Barar, A. Barzegari, Y. Omidi, Systematic evolution of ligands by exponential enrichment selection of specific aptamer for sensing of methamphetamine, Sens. Lett. 5 (3) (2013) 566–570.
[28] M. Yarbakht, M. Nikkhah, Unmodified gold nanoparticles as a colorimetric probe for visual methamphetamine detection, J. Exp. Nanosci. 11 (2015) 1–9.
[29] R. Elghanian, J.J. Storhoff, R.C. Mucic, R.L. Letsinger, C.A. Mirkin, Selective colorimetric detection of polynucleotides based on the distance-dependent optical properties of gold nanoparticles, Science 277 (5329) (1997) 1078–1081.
[30] K. Mao, Y. Chen, Z. Wu, X. Zhou, A. Shen, J. Hu, Catalytic strategy for efficient degradation of nitroaromatic pesticides by using gold nanoflower, J. Agr. Food Chem. 62 (44) (2014) 10638–10645.
[31] D. Liu, Z. Wang, X. Jiang, Gold nanoparticles for the colorimetric and fluorescent detection of ions and small organic molecules, Nanoscale 3 (4) (2011) 1421–1433.
[32] lR.R. De, M.M. Stevens, Plasmonic ELISA for the ultrasensitive detection of disease biomarkers with the naked eye, Nat. Nanotechnol. 7 (12) (2012) 821–824.
[33] Y. Mao, T. Fan, R. Gysbers, Y. Tan, F. Liu, S. Lin, Y. Jiang, A simple and sensitive aptasensor for colorimetric detection of adenosine triphosphate based on unmodified gold nanoparticles, Talanta 168 (2017) 279–285.
[34] J. Li, S. Song, D. Li, Y. Su, Q. Huang, Y. Zhao, C. Fan, Multi-functional crosslinked Au nanoaggregates for the amplified optical DNA detection, Biosens. Bioelectron. 24 (11) (2009) 3311–3315.
[35] X. Xu, D.G. Georganopoulou, H.D. Hill, C.A. Mirkin, Homogeneous detection of nucleic acids based upon the light scattering properties of silver-coated nanoparticle probes, Anal. Chem. 79 (17) (2007) 6650–6654.
[36] T.A. Taton, C.A. Mirkin, R.L. Letsinger, Scanometric DNA array detection with nanoparticle probes, Science 289 (5485) (2000) 1757–1760.
[37] D. Kim, W.L. Daniel, C.A. Mirkin, Microarray-based multiplexed scanometric immunoassay for protein cancer markers using gold nanoparticle probes, Anal. Chem. 81 (21) (2009) 9183–9187.
[38] Y.C. Cao, R. Jin, C.A. Mirkin, Nanoparticles with Raman spectroscopic fingerprints for DNA and RNA detection, Science 297 (5586) (2002) 1536–1540.
[39] J. Wang, Y. Cao, Y. Xu, G. Li, Colorimetric multiplexed immunoassay for sequential detection of tumor markers, Biosens. Bioelectron. 25 (2) (2009) 532–536.
[40] L. Song, K. Mao, X. Zhou, J. Hu, A novel biosensor based on Au@Ag core–shell nanoparticles for SERS detection of arsenic (III), Talanta 146 (2016) 285–290.
[41] R.A. Reynolds, C.A. Mirkin, R.L. Letsinger, Homogeneous, nanoparticle-based quantitative colorimetric detection of oligonucleotides, J. Am. Chem. Soc. 122 (15) (2000) 3795–3796.
[42] W. Yan, L. Yang, H. Zhuang, H. Wu, J. Zhang, Engineered "hot" core–shell nanostructures for patterned detection of chloramphenicol, Biosens. Bioelectron. 78 (2016) 67–72.
[43] J. Hao, B. Xiong, X.D. Cheng, Y. He, E.S. Yeung, A. Chem, High-throughput sulfide sensing with colorimetric analysis of single Au-Ag core-shell nanoparticles, Anal. Chem. 86 (10) (2014) 4663–4667.
[44] T. Li, Y. Li, Y. Zhang, C. Dong, Z. Shen, A. Wu, A colorimetric nitrite detection system with excellent selectivity and high sensitivity based on Ag@Au nanoparticles, Analyst 140 (4) (2015) 1076–1081.
[45] A. Shen, L. Chen, W. Xie, J. Hu, A. Zeng, R. Richards, J. Hu, Triplex Au–Ag–C core–shell nanoparticles as a novel Raman label, Adv. Func. Mater. 20 (6) (2010) 969–975.
[46] S.J. Hurst, A.K.R. Lyttonjean, C.A. Mirkin, Maximizing, D.N.A. Loading, on a range of gold nanoparticle sizes, Anal. Chem. 78 (24) (2006) 8313–8318.
[47] J.J. Wang, Y.Z. Jiang, Y. Lin, L. Wen, C. Lv, Z.L. Zhang, G. Chen, D.-W. Pang, Simultaneous point-of-care detection of enterovirus 71 and coxsackievirus B3,

Anal. Chem. 87 (21) (2015) 11105–11112.
[48] Y. Liu, Z. Wu, G. Zhou, Z. He, X. Zhou, A. Shen, J. Hu, Simple, rapid, homogeneous oligonucleotides colorimetric detection based on non-aggregated gold nanoparticles, Chem. Commun. 48 (26) (2012) 3164–3166.
[49] R.L. Hawks, C.N. Chiang, Urine testing for drugs of abuse, Nida Res. Monogr. 73 (2) (1986) 1.
[50] A.H. Oghli, E. Alipour, M. Asadzadeh, Development of a novel voltammetric sensor for the determination of methamphetamine in biological samples on the pretreated pencil graphite electrode, RSC Adv. 5 (2015) 9674–9682.
[51] Y. Aminot, X. Litrico, M. Chambolle, C. Arnaud, P. Pardon, H. Budzindki, Development and application of a multi-residue method for the determination of 53 pharmaceuticals in water, sediment, and suspended solids using liquid chromatography-tandem mass spectrometry, Anal. BioAnal. Chem. 407 (28) (2015) 8585–8604.
[52] C. Boix, M. Ibáñez, J.V. Sancho, J. Rambla, J.L. Aranda, S. Ballester, F. Hernández, Fast determination of 40 drugs in water using large volume direct injection liquid chromatography–tandem mass spectrometry, Talanta 131 (2015) 719–727.
[53] P. Gago-Ferrero, V. Borova, M.E. Dasenaki, NS. Thomaidis, Simultaneous determination of 148 pharmaceuticals and illicit drugs in sewage sludge based on ultrasound-assisted extraction and liquid chromatography–tandem mass spectrometry, Anal. BioAnal. Chem. 407 (15) (2015) 4287–4297.